Korea-Australia Rheology Journal
Vol. 16, No. 2, June 2004 pp. 85-90

Measurement of red cell deformability and whole blood viscosity using laser-diffraction slit rheometer

Sehyun Shin*, Yunhee Ku, Myung-Su Park and Jang-Soo Suh[1]
School of Mechanical Engineering, [1]Dept. of Pathological Physiology, Kyungpook National University, Daegu 702-701 Korea
(Received April 20, 2004; final revison received May 14, 2004)

Abstract

The present study investigated the deformability of red blood cells (RBC) and its effect on whole blood viscosity using a laser-diffraction slit-rheometer (LDSR). The LDSR has been recently developed with significant advances in laser-diffractometry design, operation and data analysis. While shear stress levels in a slit flow are continuously decreasing, both the deformation of red blood cells and the shear stress were simultaneously measured. Additionally, the viscosity of whole blood was measured using the LDSR. The present study found that the whole blood viscosity is strongly dependent on the RBC deformability. The less deformable the RBCs are, the higher the blood viscosity is.

Keywords : slit, deformability, RBC, diffraction, viscosity, stress

1. Introduction

Normal red blood cell (RBC) in healthy human blood readily deforms when subjected to shear stress. The deformation of RBCs plays a key role in blood circulation since they have to pass through capillaries whose diameter is smaller than their size. This RBC deformability is also known to be responsible for the surprisingly low viscosity at high shear rates in the large arteries, although whole blood consists of almost 50% of the volume of the blood cells (Chien, 1970; 1987). A slight decrease in red cell deformability may reduce the rate of entry into the capillaries and subsequently cause serious diseases such as diabetes (Attali and Vaensi, 1990), hypertension (Puniyani *et al.*, 1992), sickle cells (Usami *et al.*, 1975) and myocardial infarction. A large variety of diseases have been described in association with less deformable RBCs (Lowe *et al.*, 1988).

Various techniques in measuring the deformability of RBCs have been proposed and their comparison can be found elsewhere (Bareford *et al.*, 1985; Wang *et al.*, 1999). Typical techniques can be briefly summarized as follows: (i) *RBC filtration*: This method has been widely used in measuring RBC deformability due to its similarity and simplicity (Hanss, 1983; Koutsouris *et al.*, 1988). The deformability can be determined by measuring either the pressure built up across the membrane during a test period or the transit time related to a certain number of RBCs. There, however, is a major drawback to this method in that a calibration standard is lacking; (ii) *Ektacytometry* (Hardeman *et al.*, 1994; Schmid-Schönbein *et al.*, 1996): The principle of this technique uses laser diffraction analysis of RBCs under varying stress levels, which was developed after the work of Bessis and Mohandas (1980). Commercial instruments are LORCA® (R&R Mechatronics, Amsterdam, Netherlands) and RHEODYN-SSD® (Myrenne, Roetgen, Germany). The advantage of this technique is that cellular deformability of a number of cells can be measured rapidly using extremely small quantities of blood (less than 50 μl). (iii) *Rheoscope* (Schmid-Schönbein *et al.*, 1969; Dobbe *et al.*, 2002): It is a direct observation of the shape of RBCs under given shear stress. Other methods such as centrifugation and micropipette aspiration were also used to measure RBC deformability.

Although there are many methods and instruments for measuring deformability as described above, most of the current techniques including ektacytometry require cleaning after each measurement. In order to measure cell deformability in a clinical setting, one needs to repeat the cleaning after each measurement, which leads to a labor-intensive and time-consuming process. Hence, the current techniques are not optimal for day-to-day clinical use. Therefore, there has been a need to develop a simple and labor-free disposable element which eliminates frequent cleaning.

Recently, a new laser-diffraction slit rheometer (LDSR) was introduced to measure RBC deformability (Shin *et al.*, 2004). This device adopts a disposable element to which is in contacted with blood samples so that it can be used in

*Corresponding author: shins@wmail.knu.ac.kr

a clinical setting. One of the essential features for a LDSR is to measure both viscosity and deformability, whereas most of the current ektacytometry method cannot measure fluid viscosity. In fact, the RBC deformability is known to be a determinant of blood viscosity (Chien, 1987). Thus, the objective of this paper was to investigate the effect of the deformability on blood viscosity using the LDSR. To achieve this aim, we measured the deformability of various artificially hardened RBCs and the viscosity of the RBC suspensions with the LDSR.

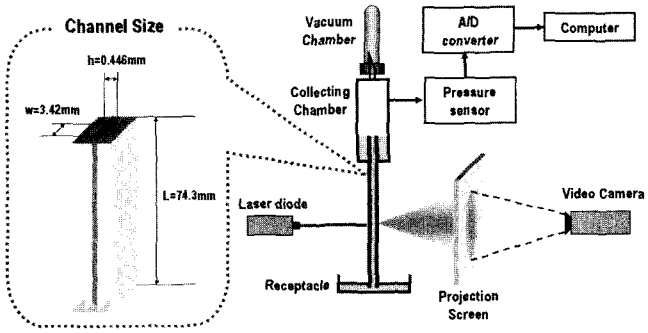

Fig. 1. Schematic diagram of a laser-diffraction slit rheometer.

2. Materials and methods

Sample preparation

Blood was obtained from normal, healthy volunteers who were not on any medications and who provided informed consent (age range 25 – 40 years and male/female participants). The blood samples used in the experiments were not pooled from more than one individual subject and all analyses were completed within 6 hours after blood collection. The samples of venous blood were drawn from the antecubital vein and collected into an EDTA containing Vacutainers (BD, Franklin Lakes, NJ). The RBCs were separated from the whole blood by centrifugation 1,200 g for 10 min. and washed with a 10 mM phosphate buffered saline (PBS; pH = 7.4; osmorality 290 mOsm/kg). The washed RBCs were then resuspended in the PBS in a range of hematocrits of 0.01 ~ 5, which were examined to obtain an optimal concentration for a laser diffraction pattern in the present slit geometry. In addition, the optimally-diluted RBC suspension was exposed to four different concentrations of glutaraldehyde (GA; Sigma, St. Louis, MO, USA) at 25°C for 30 min (0.005, 0.015, 0.02%). Following the treatment or control period, the RBCs were washed three times with phosphaste-buffered saline (PBS) pH 7.4 and resuspended in the solution of 0.14 mM Polyvinypyrrolidone (PVP, M = 360000, Sigma, St. Louis, MO, USA).

Apparatus and operation

The basic apparatus of the LDSR, containing a laser, a CCD video camera, screen, and pressure driven slit rheometry, is shown in Fig. 1. The laboratory setup also consisted of a computer. Details of the pressure-driven slit rheometry consist of a vacuum chamber, connecting needle, collecting chamber, receptacle, pressure transducer and a computer data acquisition system. With vacuum suction, the blood sample flows through the slit made of glass with a gap of 0.49 mm and a width of 3.7 mm. The glass slit integrated with a collecting chamber is designed to be disposable. The diode laser (650 nm, 5 mW) and a CCD camera (SONY-ES30) combined with a frame grabber were used to obtain a laser-diffraction pattern. The diffraction pattern is analyzed by an ellipse-fitting-program and the elongation indices (EI) are calculated for shear stress levels between 0 ~ 35 Pa. The length and gap of the slit were chosen to ensure that the friction loss in the slit was the dominant loss in the system.

Prior to the test, the atmospheric pressure (P_A) and the total volume of the vacuum chamber (V_0) are determined. Typical tests are conducted as follows: At time $t = 0$, the preset vacuum chamber is pushed into the connecting needle so that the preset chamber and the slit are opened, allowing the fluid to flow through the slit and be collected in the collecting chamber as driven by the differential pressure. As the collecting chamber is filled with the fluid, the vacuum pressure in the chamber is released. When the differential pressure reaches equilibrium with a pressure head, the test fluid stops flowing.

While the blood is flowing through the slit, a laser beam emitting from the laser diode traverses the diluted RBC suspension and is diffracted by the RBCs in the volume. The diffraction pattern projected on the screen is captured by a CCD-video camera, which is linked to a frame grabber integrated with a computer. While the differential pressure is decreasing, the RBCs change gradually from the prolate ellipsoid towards a biconcave morphology. The Elongation Index (*EI*) as a measure of the RBC deformability is determined from an isointensity curve in the diffraction pattern using an ellipse-fitting program.

The essential feature of the LDSR was the use of a precision pressure transducer (Druck, PMP4170) to measure the pressure difference between the vacuum chamber and atmosphere, $\Delta P(t)$, every 0.05 s with a resolution of 1 Pa. The instantaneous pressure was recorded in a computer data file through an analog-to-digital data acquisition system (NI DAS-16) with respect to time. From the measured pressure difference, the corresponding wall-shear stress can be determined as $\tau_w(t) = \Delta P(t)h/\{(1 + 2h/w)L\}$.

Fig. 2 shows variations of the wall shear stress over time for a RBC suspension. As shown in Fig. 2, the shear stress exponentially decreases with time since the pressure of the vacuum chamber exponentially reach atmospheric pressure due to incoming fluid from the slit. Thus, the differential pressure and the corresponding wall shear stress are exponentially decreasing with time. Typically, it took approx-

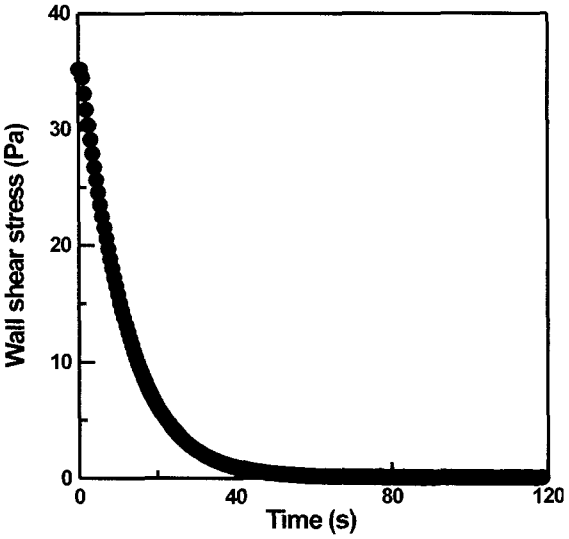

Fig. 2. Shear stress variation versus time for blood sample.

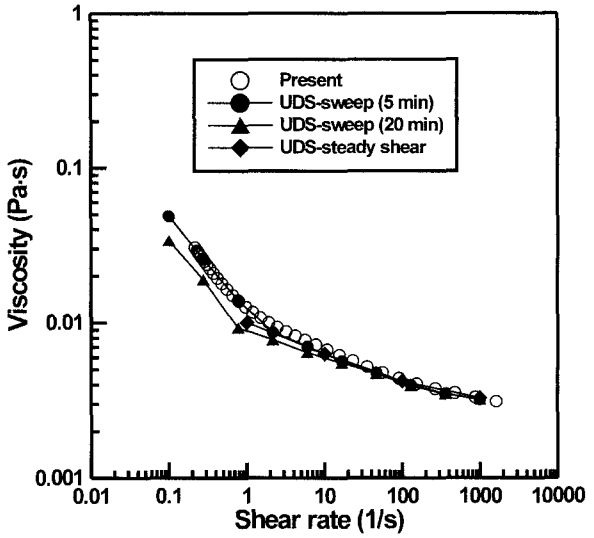

Fig. 3. Viscosity measurement (log-log scale) for blood sample with a rotating viscometer and LDSR.

imately 2 min to reach an asymptote for the resuspended fluid as shown in Fig. 2. It is worth noting that if the initial pressure in the vacuum chamber would be lowered, the maximum shear stress can easily be increased.

Mathematical principles

A detailed description of the stress-shear rate relation can be found in a previous study (Shin *et al.*, 2002). A brief description is as follows: In deriving the stress-shear rate relation in the slit rheometer, the important assumptions are 1) a fully developed, isothermal, laminar flow; 2) no slip at the walls; and 3) air in the vacuum chamber as an ideal gas. On the assumption that the product of pressure $P(t)$ and volume $V(t)$ in the vacuum chamber at time t is constant, $P_iV_i = P(t)V(t)$, where subscript i represents the initial state of the experiment, the instantaneous pressure $P(t)$ is recorded in the computer file. The flow rate at time t can be obtained as $Q(t) = \frac{d}{dt}\left(\frac{P_iV_i}{P(t)}\right)$.

On the other hand, the pressure difference through a slit can be expressed as $P = \{P_AP(t) - \rho gL\}$ and the corresponding shear stress is determined from the following equation.

$$\tau_w(t) = \frac{\Delta P(t)h/L}{(1+(2h)/w)} \tag{1}$$

The shear rate at the slit wall is obtained from the classical Weissenberg-Rabinowitsch equation (Macosko, 1993)

$$\dot{\gamma}_w(t) = -\left.\frac{dv_z}{dz}\right|_w = \frac{1}{3}\dot{\gamma}_{aw}\left[2+\frac{d\ln Q}{d\ln \tau_w}\right] \tag{2}$$

where $\dot{\gamma}_{aw}$ is $6Q/wh^2$. Then, the viscosity can be easily determined as $\eta = \tau_w/\dot{\gamma}_w$. The dimensions of the slit were chosen to ensure that the friction loss in the slit was significantly greater than the loss in other parts of the system (Shin *et al.*, 2004). In addition, wall slip for RBC suspensions may be considered in correcting the measured apparent viscosity (Chang *et al.*, 2003).

For calibration purposes of the slit rheometer, a whole blood sample was measured and the results were compared with those measured by a rotating viscometer (Physica model UDS-200, Parr Physica, Inc.). Fig. 3 shows the viscosity results obtained with the blood sample at 37°C, respectively. Open circle symbols indicate the viscosity data measured with the LDSR; solid symbols indicate those measured with the rotating viscometer. It is worth to note that the viscosity measurement with the LDSR is similar to the sweep mode measurement for the rotating viscometer. The LDSR results show excellent agreement (less than 3.8%) with those from the rotating viscometer with sweep mode (5 min) over a range of shear rates (10^{-1} ~ 10^3 1/s). However, the LDSR results show a little difference from the rotating viscometer with sweep mode (20 min) and steady shear mode. In fact, the viscosity measuring method with the LDSR is similar to the sweep mode for the rotating viscometer, which measures the viscosity during unsteady process. However, these results occur in the low range of shear rate as shown in Fig. 3. This fact implies that the transient viscosity measurement may be affected by aggregation characteristics, which is also dependent on deformability. It is worth to further study the blood viscosity related with cell aggregation and deformation.

3. Results and discussion

Fig. 4 compares the diffraction patterns captured at two different conditions ($\tau_w = 0.2$ Pa and 35 Pa) measured by the LDSR. At a high shear stress condition, the diffraction

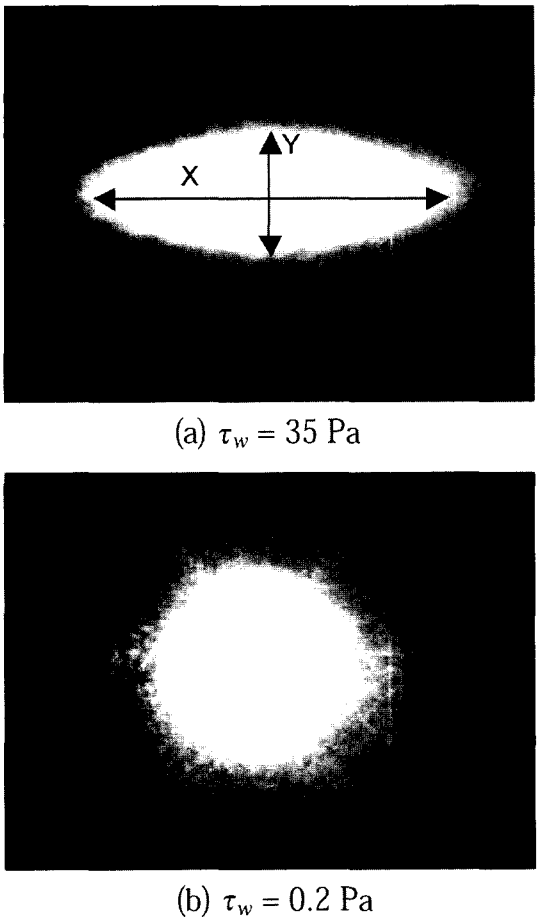

Fig. 4. Laser diffraction patterns at two different shear conditions.

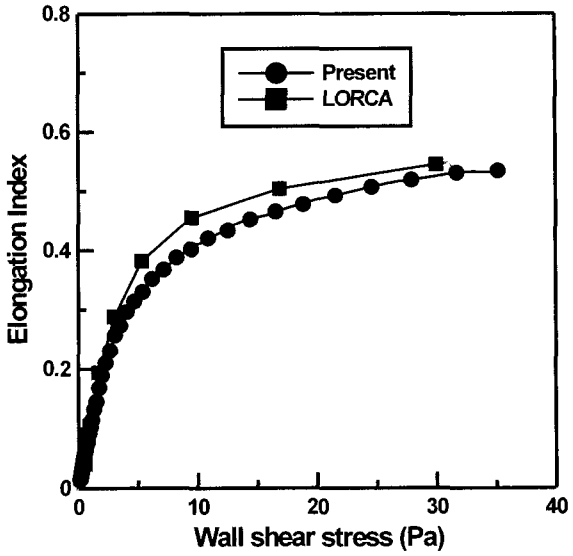

Fig. 5. Elongation Index versus wall shear stress for control blood.

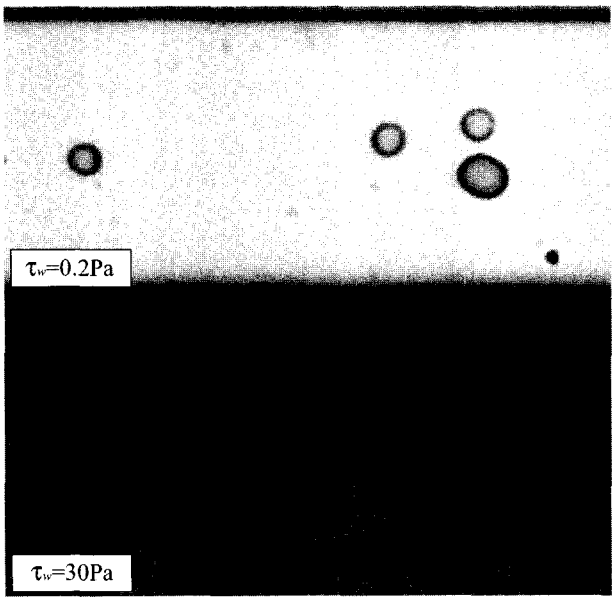

Fig. 6. Cell images drifting in micro-channel.

pattern shows a prolate ellipsoid shape since the RBCs were elongated. When eliminating the shear stress, however, the diffraction pattern recoils to the original circular shape. As described earlier, the Elongation Index (*EI*) as a measure of RBC deformability is determined from an isointensity curve in the diffraction pattern using an ellipse-fitting program. The EI is defined as $(X - Y)/(X + Y)$, where X and Y are the major and minor axes of the ellipse, respectively.

Fig. 5 compares the mean values of *EI* for normal erythrocytes measured with the LDSR and LORCA as a function of shear stress applied. The rectangle symbols indicate the EI measured with the LORCA; and circle symbols indicate those measured with the present LDSR. Compared with these results, the test results give about a 8.3% error across the entire shear stress range. These values were the same as compared with those of other instruments (Wang *et al.*, 1999). The deviation shown in Fig. 5 may be due to the generic flow characteristics between the slit flow and rotational Couette flow. In fact, the latter has more of a uniform shear profile than the former.

In addition, the present results measured with the LDSR were compared with rheoscopical measurements. The present study conducts a flow visualization experiment in a micro-channel (40 μm × 200 μm × 20 mm) using an inverted microscope and a high speed camera. Focal point was set at the quarter of the channel gap apart from the top wall. Pictures were taken every 0.5 ms. Captured images are digitized and analyzed off-line by dedicated software. Cells are automatically located in each image and the contour of each cell projection is fitted by an ellipse, allowing to estimate the major (X) and minor (Y) axes of the cell.

Fig. 6 shows a series of RBC images drifting in the micro-channel at two different wall shear stress conditions (τ_w = 0.2 and 35 Pa). Comparing these results of rheoscopical and diffraction analyses, it was observed that there

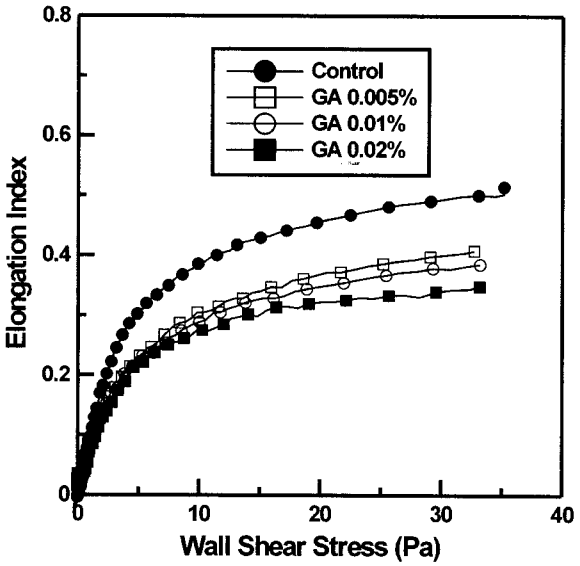

Fig. 7. Elongation Index versus wall shear stress for four different blood samples.

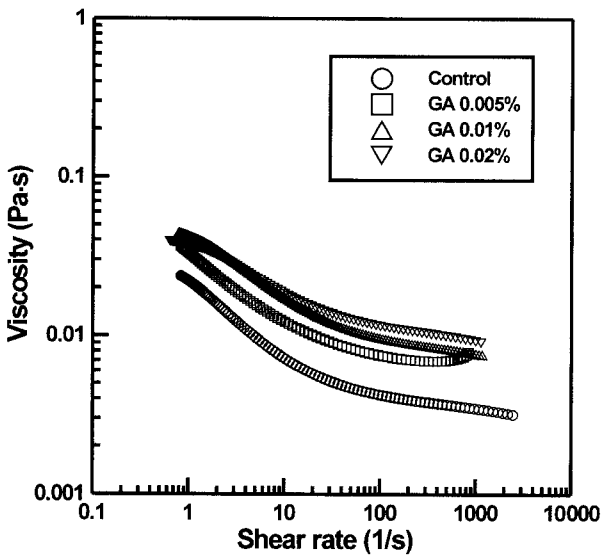

Fig. 8. Blood viscosity versus shear rate for differently hardened RBC suspensions.

was also good correlation of *EI* values given by the two instruments. However, these rheoscopical results cannot be representative for RBC deformability due to the small number of RBC images and currently-developing image processing software. Dobbe *et al.* (2002) used approximately 2,000 valid cell images to represent the RBC deformability. Thus, the present rheoscopical apparatus was developed as a proof of principle to measure RBC deformability.

Meanwhile, the present study measured the RBC deformability with the present slit-flow ektacytometry. In order to vary the deformability of the RBCs, the RBCs were exposed to three different concentrations (0.005, 0.01 0.02%) of glutaraldehyde (GA). It has been known that the higher the concentration of GA uses, the less deformable the RBCs become. Fig. 7 shows the Elongation Index (*EI*) along a shear stress for control and hardened RBCs. As shown in Fig. 7, the controlled RBCs show the highest plateau value of an *EI* at a high shear stress. As the levels of the GA concentration increased, the *EI* values decreased.

Meanwhile, the present laser-diffraction slit rheometer is able to measure blood viscosity as well as RBC deformability. Thus, the effect of RBC deformability on the whole blood viscosity was investigated using the same LDSR. Fig. 8 shows blood viscosity for various RBCs having different deformability. The more hardened cells are, the higher the blood viscosity is. It is observed that deformability affects high-shear viscosity more than low-shear viscosity. However, the variation of the low-shear viscosity is not negligible in Fig. 8. In fact, it is commonly known that the low shear viscosity is strongly dependent on RBC aggregation, which is also affected by cellular properties including RBC deformability (Baskurt and Meiselman, 2003). Thus, the deformability-dependent blood viscosity shown in Fig. 8 should be interpreted by considering RBC aggregation, shearing condition, and RBC volume concentration (Chien, 1970).

4. Conclusion

The deformability of normal and hardened RBCs was measured with the newly developed instrument (LDSR) and the results showed a correlation with those of a commercial ektacytometer (LORCA), which are based on laser diffraction. Furthermore, the viscosity of the corresponding RBC suspensions was successfully measured with a LDSR. The RBC suspension viscosity was strongly dependent on the RBC deformability over a range of shear rates. The LDSR appeared to offer interesting possibilities as a clinical device in the diagnosis of blood viscosity as well as RBC deformability.

Nomenclature

EI	: elongation index
h	: slit gap, [m]
L	: slit length, [m]
P	: pressure, [kPa]
Q	: volume flow rate, [m^3/s]
V	: volume, [m^3]
v	: velocity, [m/s]
t	: time, [s]
w	: slit width, [m]
ΔP	: pressure difference between atmosphere and the vacuum chamber ($= P_A - P_{vc}$)

Greek Symbols

ρ : density, [kg/m^3]
η : non-Newtonian viscosity, [Pa · s]
$\dot{\gamma}$: shear rate, [s^{-1}]
τ : shear stress, [Pa]

Subscripts

A : atmosphere
vc : vacuum chamber
w : wall

Acknowledgments

This work was supported by a Grant from the National Research Laboratory of the Ministry of Science and Technology, Korea.

References

Attali, J.R. and P. Vaensi, 1990, Diabetes and hemorheology, *Diabetes Metab* **16**, 1.

Bareford, D., P.C.W. Stone, N.M. Calwell, H.J. Meiselman and J. Stuart, 1985, Comparison of instruments for measurement of erythrocyte deformability, *Clin. Hemorheol.* **5**, 311.

Baskurt, O.K. and H.J. Meiselman, 2003, Blood rheology and hemodynamics, *Seminars in thrombosis and hemostasis* **29**, 435.

Bessis, M. and N. Mohandas, 1975, A diffractometric method for the measurement of cellular deformability, *Blood Cells* **1**, 307.

Bessis, M., N. Mohandas and C. Deo, 1980, Automated ektacytometry: A new method of measuring red cell deformability and cell indices, *Blood cells* **6**, 315.

Chang, G.S., J.S. Koo and K.W. Song, 2003, Wall slip of Vaseline in steady shear rheometry, *Korea-Australia Rheol. J.* **15**, 55.

Chien, S., 1970, Shear dependence of effective cell volume as a determinant of blood viscosity, *Science* **168**, 977

Chien, S., 1978, Principles and techniques for assessing erythrocyte deformability, in Red Cell Rheology, ed. M. Bessis, S.B. Shohet & N. Mohandas, 71 Springer-Verlag, Berlin.

Chien, S., 1987, Red cell deformability and its relevance to blood flow, *Annu. Rev. Physiol.* **49**, 177.

Dobbe, J.G.G., M.R. Hardeman, G.J. Streekstra, J. Strackee, C. Ince and C.A. Grimbergen, 2002, Analyzing Red Blood Cell-Deformability Distributions, *Blood Cells, Molecules, and Diseases* **28**, 373.

Hanss, M., 1983, Erythrocyte filterability measurement by the initial flow rate method, *Biorheology* **20**, 199.

Hardemann, M.R. and P.T. Goedhart, 1992. Interrelationship of changes in hemorheological parameters induced by low osmolar radio-contrast media, *Clin. Hemorheol.* **12**, 381.

Hardeman, M.R., P.T. Goedhart, J.G.G. Dobbe and K.P. Lettinga, 1994, Laser-assisted optical rotational cell analyser (LORCA): A new instrument for measurement of various structural hemorheological parameters, *Clin. Hemorheol.* **14**, 605.

Holman, R.C., C.A. Herron and P. Sinnock, 1983, Epidemiologic Characteristics of Mortality from Diabetes with Acidosis or Coma, United States, 1970-78, *American Journal of Public Health* **73**, 1169.

Lowe, G., 1988, Clinical Blood Rheology. CRC Press, Boca Raton, FL.

Macosko, C.W., 1993, Rheology: Principles, Measurements, and Applications, VCH, New York.

Puniyani, R.R., R. Ajmani and P.A. Kale, 1992, Risk factors evaluation in some cardiovascular diseases, *J. Biomed. Eng.* **13**, 441.

Shin, S., D.Y. Keum and Y.H. Ku, 2002, Blood Viscosity Measurement Using a Pressure-Scanning Capillary Viscometer, *KSME Int. J.* **16**, 1719.

Shin, S., Y.H. Ku, M.S. Park, S.Y. Moon, J.H. Jang and J. S. Suh, 2004, Laser-diffraction slit rheometer to measure red blood cell deformability, *Rev. Sci. Instr.* **75**, 559.

Shin, S., S.W. Lee and Y.H. Ku, 2004, Measurements of blood viscosity using a pressure-scanning slit viscometer, *KSME Int. J.*, **18**, 1036.

Skovborg, F., A.V. Nielsen, J. Schlichtkrull and J. Ditzel, 1966, Blood viscosity in diabetics patients, *Lancet* **1**, 129.

Usami, S., S. Chien and J.F. Bertles, 1975, Deformability of sickle cells as studied by microseiving, *J. Lab. Clin. Med.* **86**, 274.

Wang, X., H. Zhao, F.Y. Zhuang and J.F. Stoltz, 1999, Measurement of erythrocyte deformability by two laser diffraction methods, *Clinical Hemorheology and Microcirculation* **21**, 291.